

## Altering Na-ion Solvation to regulate Dendrite growth for a Reversible and Stable Room-temperature Sodium-Sulfur Battery

Chhail Bihari Soni<sup>1</sup>, Saheb Bera<sup>2</sup>, Sungjemmenla<sup>1</sup>, Mahesh Chandra<sup>1</sup>, Vineeth S.K.<sup>1,3</sup>, Sanjay Kumar<sup>1</sup>, Hemant Kumar<sup>2\*</sup> and Vipin Kumar<sup>1,3\*</sup>

<sup>1</sup>Department of Energy Science and Engineering, Indian Institute of Technology Delhi, Hauz Khas, New Delhi, 110016, India

<sup>2</sup>School of Basic Sciences, Indian Institute of Technology Bhubaneswar, Odisha, 752050, India

<sup>3</sup>University of Queensland–IIT Delhi Academy of Research (UQIDAR), Indian Institute of Technology Delhi, Hauz Khas, New Delhi 110016, India

\*Email- [heman@iitbbs.ac.in](mailto:heman@iitbbs.ac.in), [vkumar@dese.iitd.ac.in](mailto:vkumar@dese.iitd.ac.in)

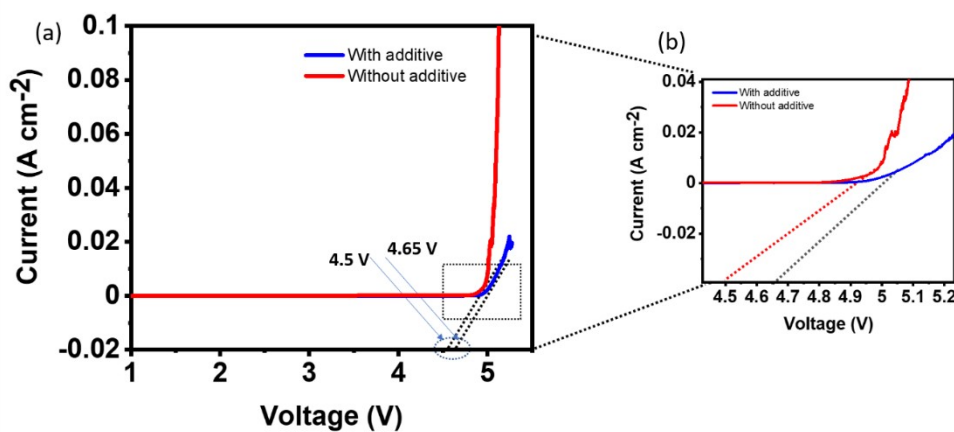


Fig. S1 Linear sweep voltammetry curve for electrolyte with additive and without additive. Na metal used as counter electrode whereas stainless steel used as working electrode

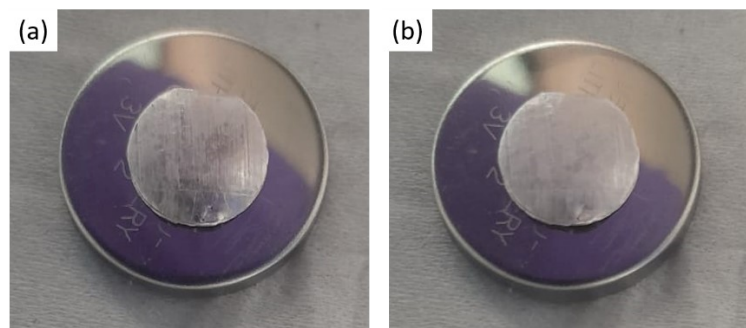


Fig. S2 Digital micrographs of a) a bare sodium metal, and b) sodium metal upon contact with NaI additive containing electrolyte. The sodium metal loses its luster; however, no apparent color change is caused by the NaI additives.

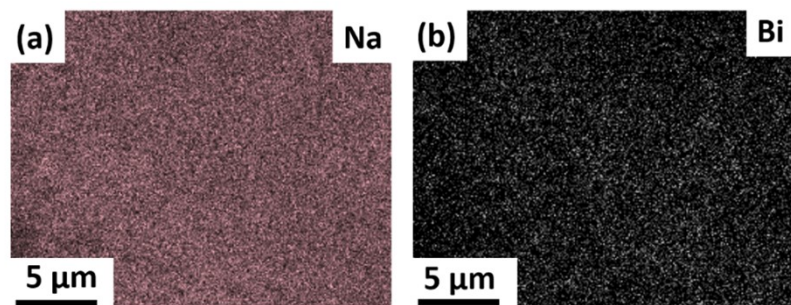


Fig. S3 EDX images of sodium metal anode top surface with additive. Here, Na and Bi, with Na comprising 68% and Bi 23% of the elemental composition on the metal anode

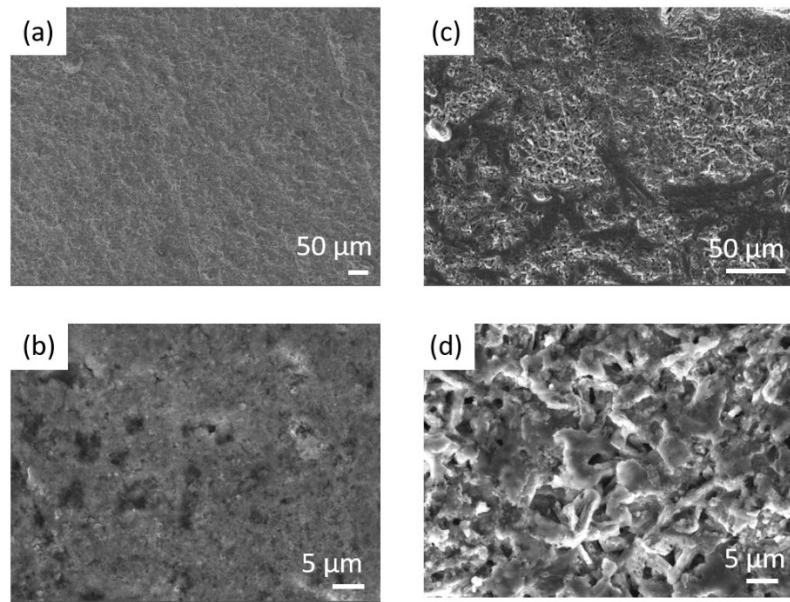


Fig. S4 FESEM images of Cu working electrode from half cells after 50 striping/plating cycles at  $1 \text{ mA cm}^{-2}$  current density and  $1 \text{ mAh cm}^{-2}$  capacity, while stripped to 1 V. (a, b) with additive (c, d) without additive

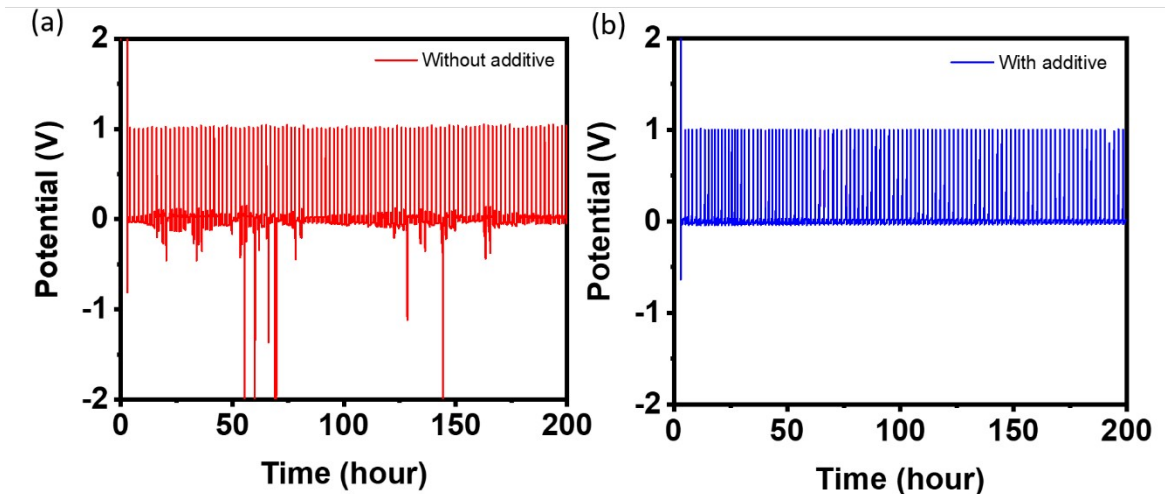


Fig. S5 Voltage vs time plots for Na//Cu half cells (a) without additive and (b) with additive at  $1 \text{ mA cm}^{-2}$  current density,  $1 \text{ mA h cm}^{-1}$  specific capacity and stripping up to 1 V.

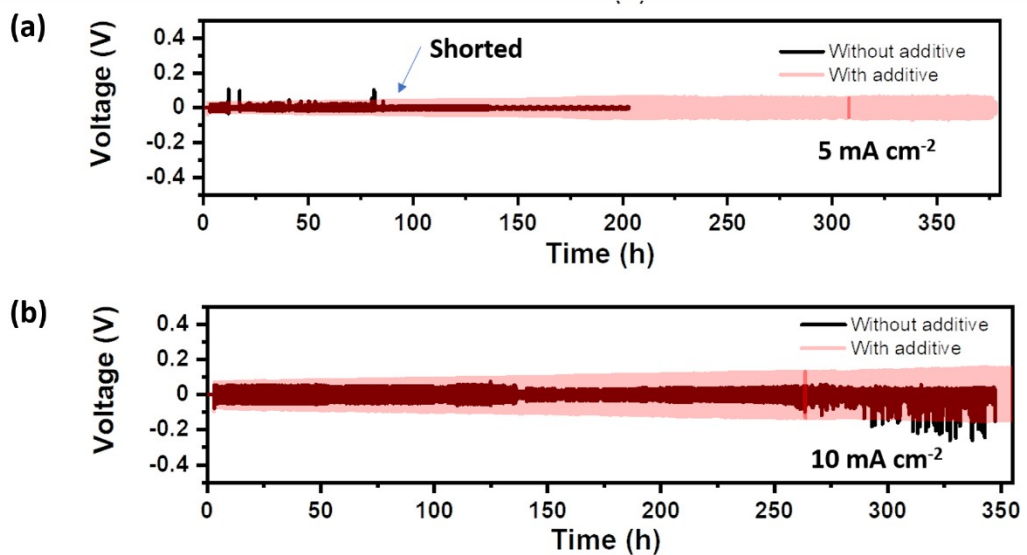


Fig. S6 (a) Stripping plating cycling performance of Na//Na symmetric cell at  $5 \text{ mA cm}^{-2}$  current density and  $1 \text{ mA h cm}^{-2}$  capacity (b) at  $10 \text{ mA cm}^{-2}$

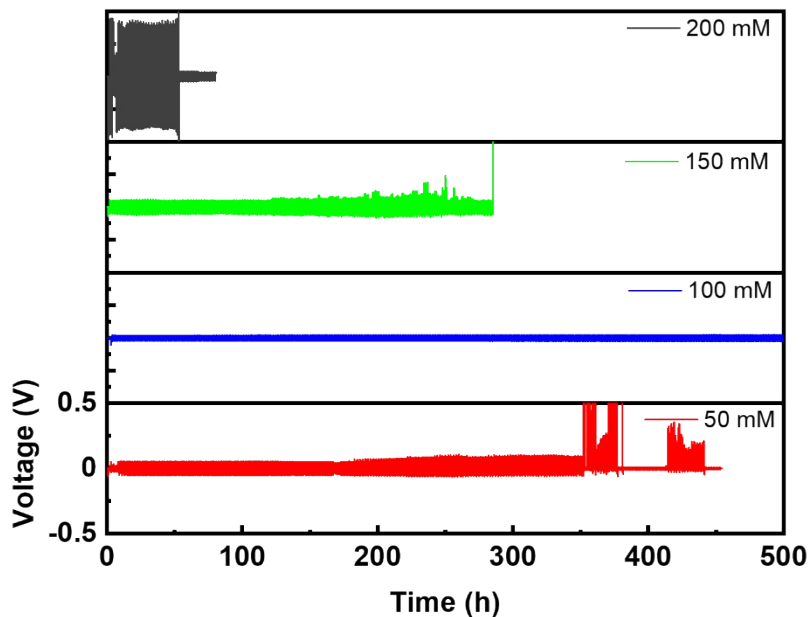


Fig. S7 Additive concentration optimization in Na//Na symmetric cell at  $1 \text{ mA cm}^{-2}$  current density. Concentration is varying from 50 to 200 mM.

Table-S1 Cyclic performance analysis of Na//Na symmetric cells with different types of additives.

Cell type	Salt	Solvent	Additive	Current density (mA cm <sup>-2</sup> )	Capacity (mA h cm <sup>-2</sup> )	Overpotential (mV)	Cycle life (h)
<b>Na//Na (This work)</b>	<b>1 M NaOTf</b>	<b>Diglyme</b>	<b>100 mM BiI<sub>3</sub></b>	<b>1</b>	<b>1</b>	<b>90</b>	<b>1600</b>
Na//Na <sup>1</sup>	1 M NaPF <sub>6</sub>	EC/PC	FEC	1	1	100	100
Na//Na <sup>2</sup>	1 M NaPF <sub>6</sub>	Diglyme	0.033 M Na <sub>2</sub> S <sub>6</sub>	2	1	38	400
Na//Na <sup>3</sup>	1 M NaClO <sub>4</sub>	EC/DEC	0.05 M SnCl <sub>2</sub>	0.5	1	100	500
Na//Na <sup>4</sup>	4 M NaFSI	DMC	1% SbF <sub>3</sub>	0.5	0.5	25	1000
Na//Na <sup>5</sup>	1 M NaTFSI	FEC	0.75 % NaAsF <sub>6</sub>	0.5	1	500	350
Na//Na <sup>6</sup>	2 M NaPF <sub>6</sub>	DME/FE PE	1% SbF <sub>3</sub>	0.5	0.5	200	1200
Na//Na <sup>7</sup>	0.3 M NaPF <sub>6</sub>	EC/PC	Acetamide (BSTFA)	0.5	0.5	120	350
Na//Na <sup>8</sup>	1 M NaOTf	Diglyme	50 mM 9-Fluorenone	1	1	25-30	1200
Na//Na <sup>9</sup>	1 M NaPF <sub>6</sub>	EC/PC	2% TMDT	0.5	1	400	450
Na//Na <sup>10</sup>	0.8 M NaPF <sub>6</sub>	TMP/FE C (7:3)	DTD as co-solvent	0.5	1	200	1350

Na/Na <sup>11</sup>	1 M NaPF <sub>6</sub>	EC/PC	Perfluorobenzene	1	1	600	300
Na/Na <sup>12</sup>	1 M NaPF <sub>6</sub>	VC	N-methyl-N-(trimethylsilyl)trifluoroacetamide	0.1	0.1	400	800

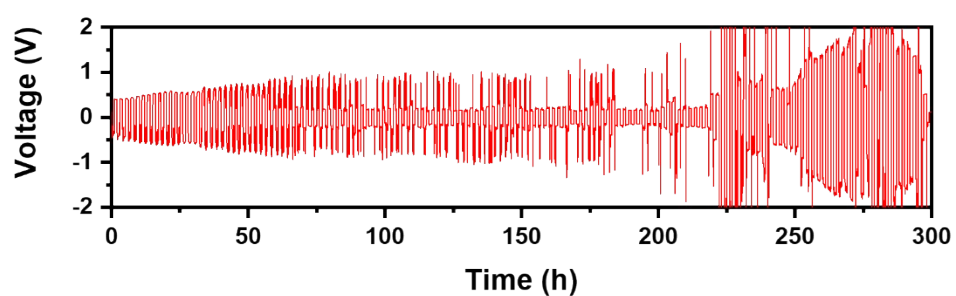


Fig. S8 Na//Na symmetric cell cycling performance in ester electrolyte (EC/DMC) at 1 mA cm<sup>-2</sup> current density and 1 mAh cm<sup>-2</sup> capacity.

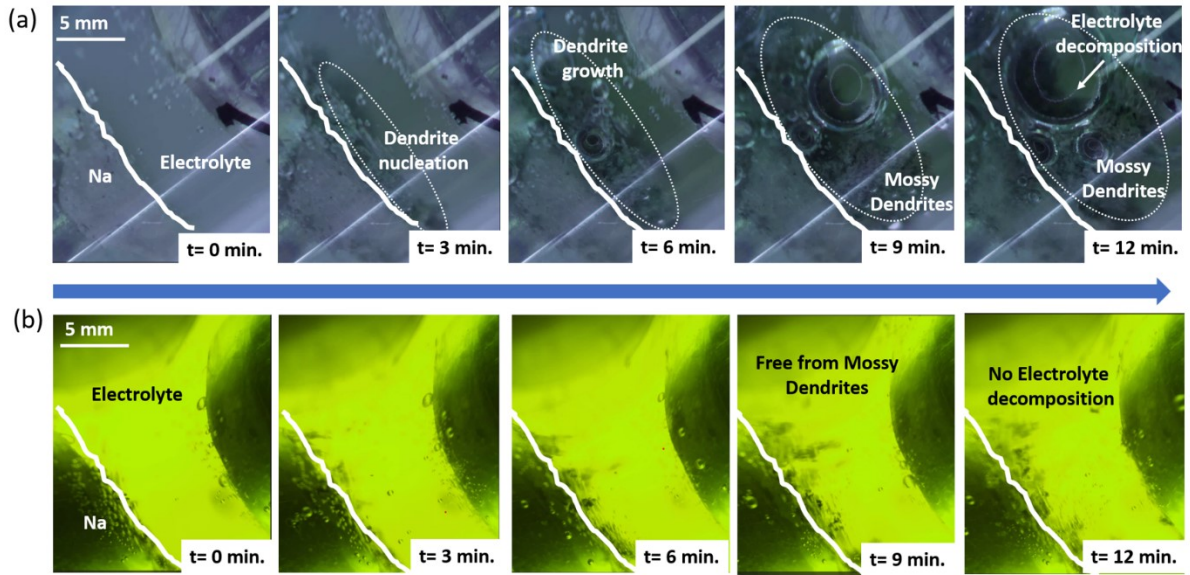


Fig. S9 In-situ optical testing for visualizing dendrite growth pattern over sodium metal anode  
(a) In conventional electrolyte without additive with mossy dendrites and bubble formation (b)  
In additive based electrolyte after a different span of time at  $5 \text{ mA cm}^{-2}$  current density.

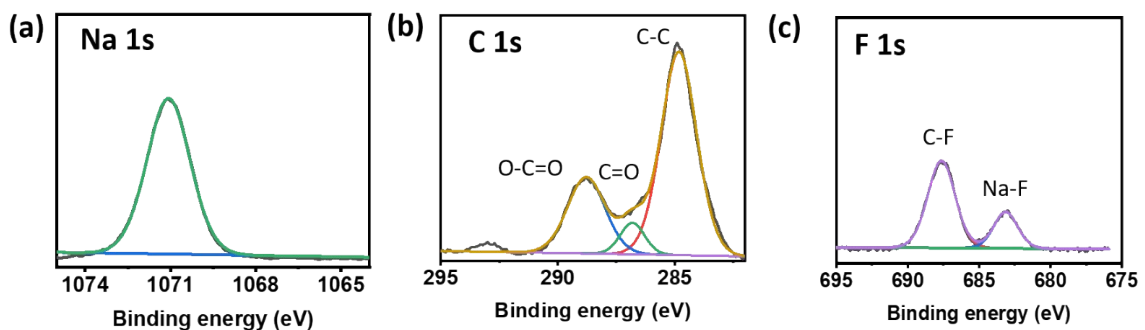


Fig. S10 XPS spectra of reference Na metal anode after cycling (a) Na 1s (b) C 1s (c) F 1s

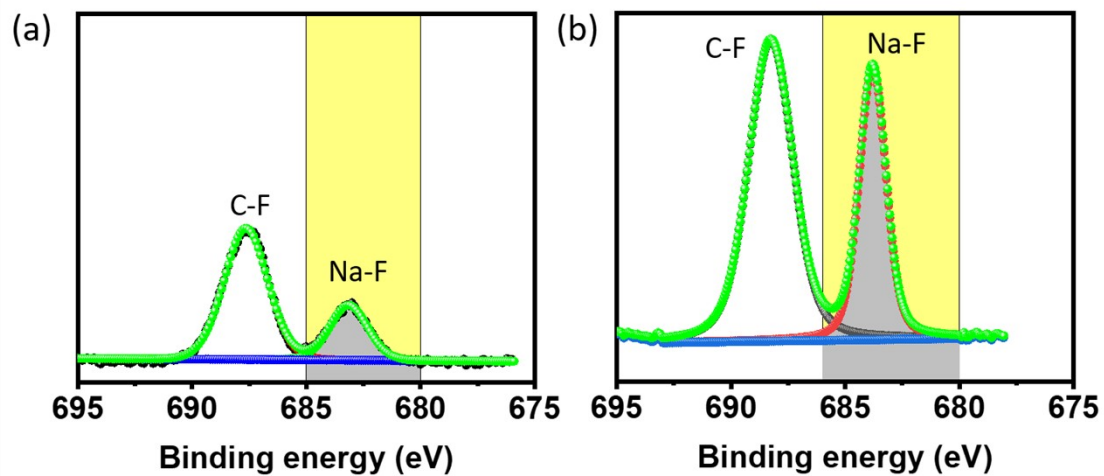


Fig. S11 (a) XPS spectra for F 1s from sodium metal anode in reference electrolyte after cycling  
(b) XPS spectra for F 1s from sodium metal anode in additive based electrolyte after cycling

Table-S2 XPS data tabulated in the form of elements, peak position, peak assignment and possible species

Element	Peak position	Peak assignment	Species
C	289.1/286.4/284.8 eV	O-C=O/C=O/C-C	NaSO <sub>3</sub> CF <sub>3</sub> /RC <sub>2</sub> Na
O	535.6/532.5/531.1	O-H/Na-O/Na-C	NaOH/Na <sub>2</sub> O/Na <sub>2</sub> CO <sub>3</sub>
Na	1071	Na-F/Na-O	NaF/Na <sub>2</sub> O
I	630.59/619.09	I 3d <sub>5/2</sub> / I 3d <sub>3/2</sub>	NaI
Bi	166.72/163.64/16 1/158.4	Bi 4f <sub>5/2</sub> (Bi <sub>2</sub> O <sub>3</sub> )/Bi 4f <sub>5/2</sub> / Bi 4f <sub>7/2</sub> (Bi <sub>2</sub> O <sub>3</sub> )/Bi 4f <sub>7/2</sub>	Na <sub>3</sub> Bi / Bi <sub>2</sub> O <sub>3</sub>
F	688.25/683.79 eV	C-F/Na-F	NaSO <sub>3</sub> CF <sub>3</sub> /NaF
S	170.33/169.02 eV	S 2p <sub>1/2</sub> / S 2p <sub>3/2</sub>	NaSO <sub>4</sub>

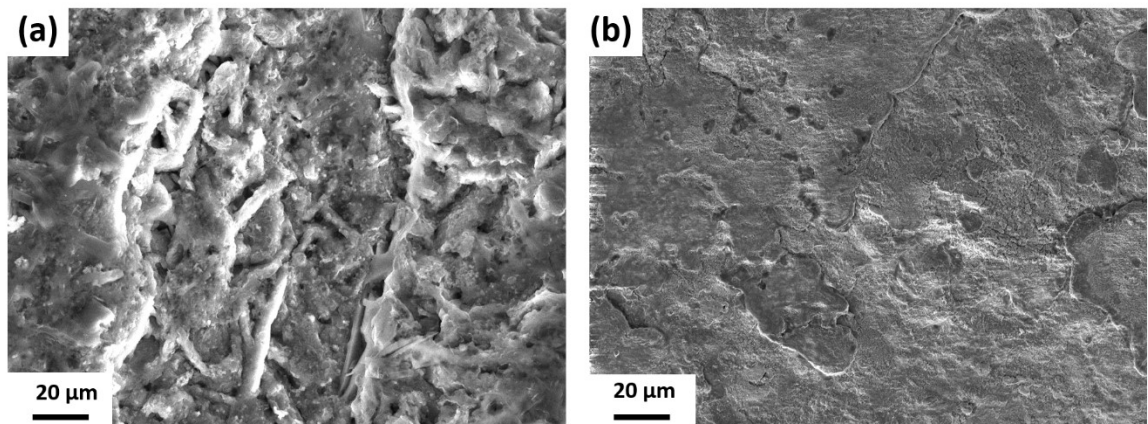


Fig. S12 FESEM images of sodium metal surface after 50 plating/stripping cycles in symmetric cell configuration (a) without additive (b) with additive

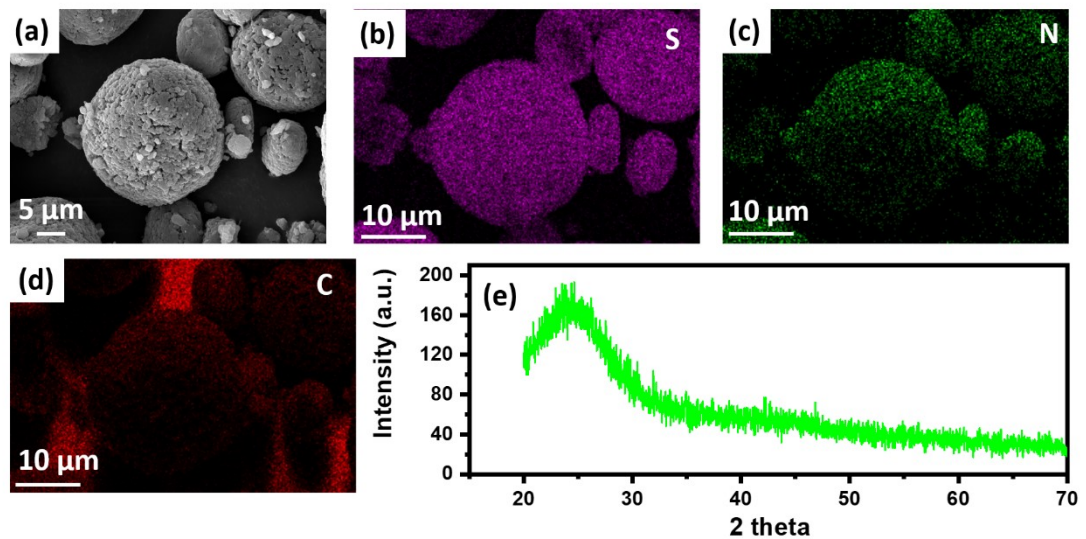


Fig. S13 (a) FESEM image of as synthesized SPAN material (b-c) corresponding EDX images (e) XRD spectra of the SPAN material

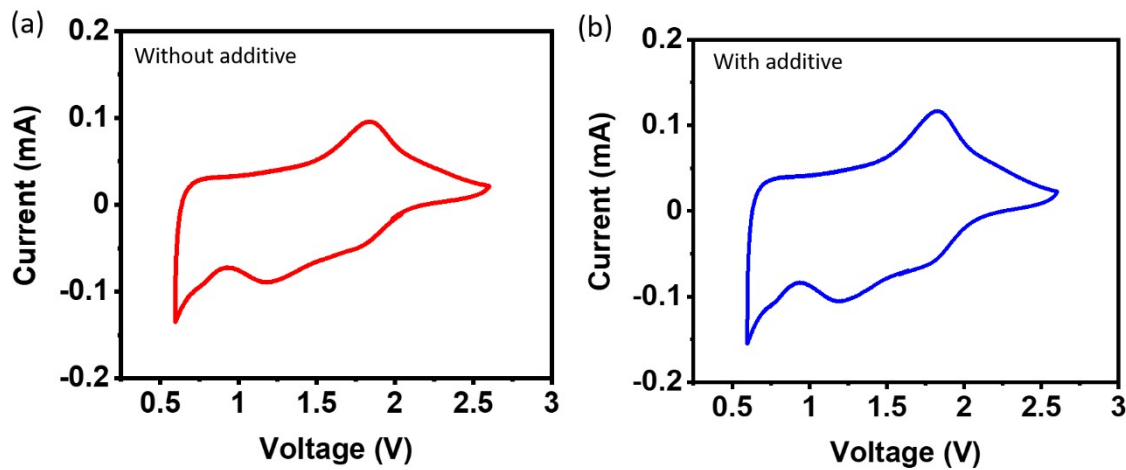


Fig. S14 (a) Cyclic voltammetry curves for Na-SPAN full cells without additive (b) with additives. CV was captured at  $0.1 \text{ mA s}^{-1}$  scan rate.

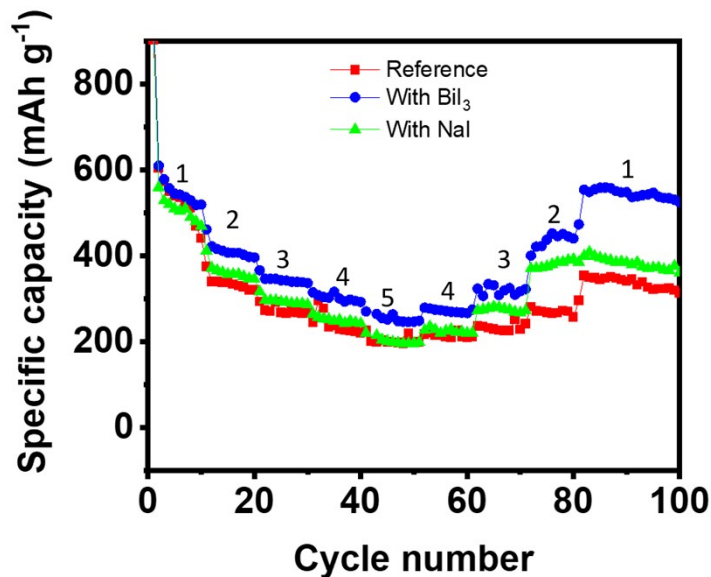


Fig. S15 Rate performance analysis for Na//SPAN full cells with  $\text{BiI}_3$ ,  $\text{NaI}$  and reference electrolyte. Where 1-5 corresponds to  $160 \text{ mA g}^{-1}$ ,  $320 \text{ mA g}^{-1}$ ,  $640 \text{ mA g}^{-1}$ ,  $800 \text{ mA g}^{-1}$ , and  $1000 \text{ mA g}^{-1}$  current density, respectively

## References

- 1 M. Han, C. Zhu, T. Ma, Z. Pan, Z. Tao and J. Chen, *Chem. Commun.*, 2018, **54**, 2381–2384.
- 2 H. Wang, C. Wang, E. Matios and W. Li, *Angew. Chemie*, 2018, **130**, 7860–7863.
- 3 X. Zheng, H. Fu, C. Hu, H. Xu, Y. Huang, J. Wen, H. Sun, W. Luo and Y. Huang, *J. Phys. Chem. Lett.*, 2019, **10**, 707–714.
- 4 W. Fang, H. Jiang, Y. Zheng, H. Zheng, X. Liang, Y. Sun, C. Chen and H. Xiang, *J. Power Sources*, 2020, **455**, 227956.
- 5 S. Wang, W. Cai, Z. Sun, F. Huang, Y. Jie, Y. Liu, Y. Chen, B. Peng, R. Cao, G. Zhang and S. Jiao, *Chem. Commun.*, 2019, **55**, 14375–14378.
- 6 W. Fang, R. Jiang, H. Zheng, Y. Zheng, Y. Sun, X. Liang, H. F. Xiang, Y. Z. Feng and Y. Yu, *Rare Met.*, 2021, **40**, 433–439.
- 7 R. Jiang, L. Hong, Y. Liu, Y. Wang, S. Patel, X. Feng and H. Xiang, *Energy Storage Mater.*, 2021, **42**, 370–379.
- 8 C. Bihari, S. Bera, S. K. Vineeth, H. Kumar and V. Kumar, *J. Energy Storage*, 2023, **71**, 108132.
- 9 M. Zhu, Y. Zhang, F. Yu, Z. Huang, Y. Zhang, L. Li, G. Wang, L. Wen, H. K. Liu, S. X. Dou and C. Wu, *Nano Lett.*, 2021, **21**, 619–627.
- 10 M. Zhu, L. Li, Y. Zhang, K. Wu, F. Yu, Z. Huang, G. Wang, J. Li, L. Wen, H. K. Liu, S. X. Dou, Y. Yu and C. Wu, *Energy Storage Mater.*, 2021, **42**, 145–153.
- 11 C. Zhu, D. Wu, Z. Wang, H. Wang, J. Liu, K. Guo, Q. Liu and J. Ma, *Adv. Funct. Mater.*, 2024, **34**, 2214195.
- 12 J. Ma, M. Yu, M. Huang, Y. Wu, C. Fu, L. Dong, Z. Zhu, L. Zhang, Z. Zhang, X. Feng and H. Xiang, *Small*, 2024, **20**, 1–13.